# Disentangling ultrafast electronic and structural dynamics with X-ray lasers

Eric Collet, Marco Cammarata

CONCEPT

# Disentangling ultrafast electronic and structural dynamics with X-ray lasers

Eric Collet*[a] and Marco Cammarata[a]

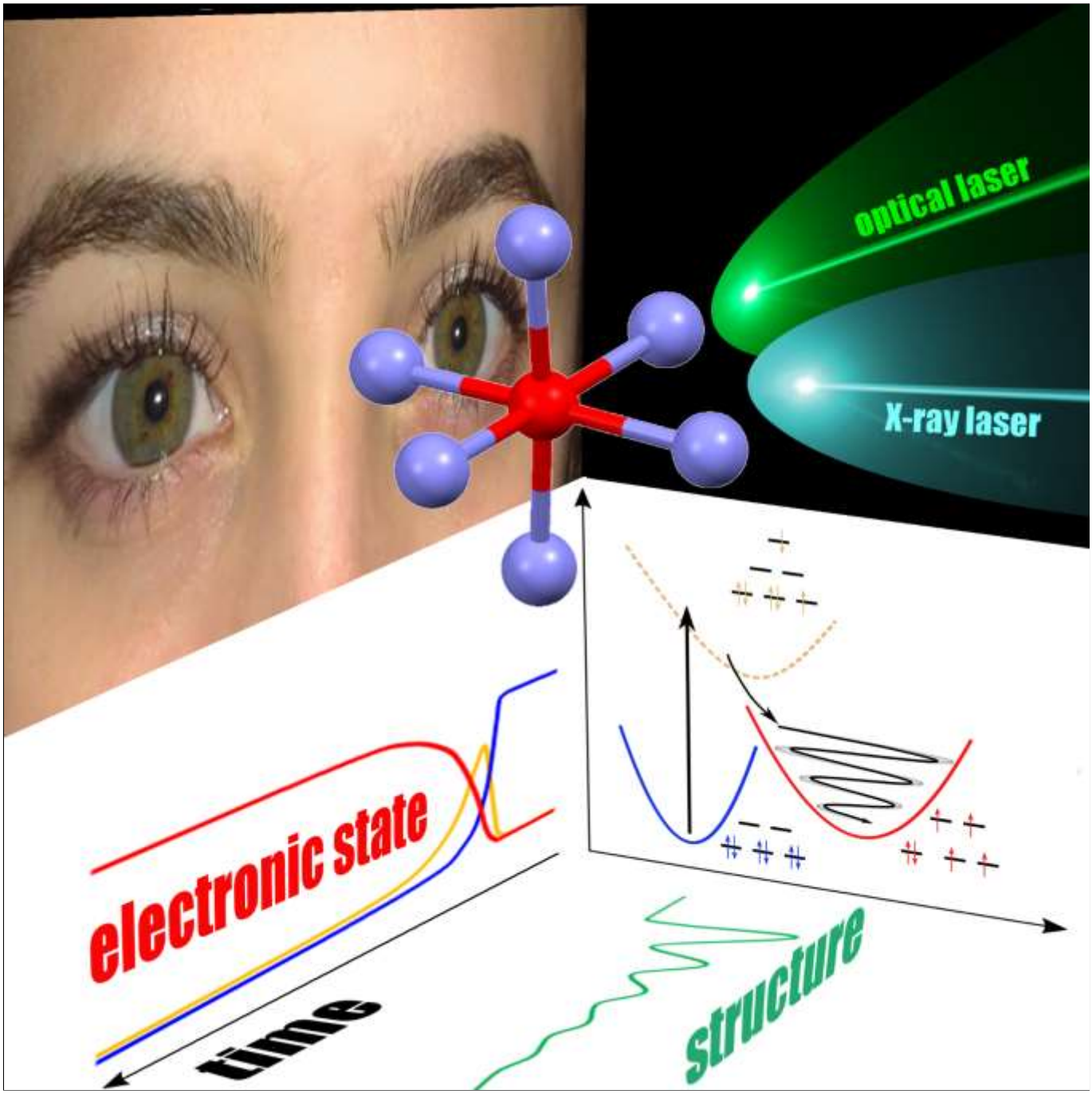

**Abstract:** Directing the functionality of molecules, materials and biophysical systems is challenging both from fundamental and applied standpoints. For example, understanding the elementary processes responsible for light-induced transformations require watching electronic and structural reorganizations on their intrinsic timescales. The X-ray free electron lasers (X-FEL) represent a new generation of incredibly short and ultra-bright X-ray source, which open new possibilities for developing the multidisciplinary field of ultrafast science. Experiments around X-FEL provide probes, sensitive to electronic and structural reorganizations, able to monitor transformations on the femtosecond timescale (1fs=$10^{-15}$s). Recent years have seen terrific successes in providing a detailed view on light-induced processes, compared to what was understood from conventional optical pump-probe spectroscopy. This Concept article aims at illustrating, through recent studies mainly focussing on light-induced excited spin state trapping, how these X-FEL based techniques can help understanding light-activated functions, by monitoring elementary electronic and structural processes that may occur beyond the Born–Oppenheimer approximation.

## 1. Introduction

Molecular transformations, at the heart of chemistry and emergence of functions of materials, involve subtle and coupled changes of electronic and nuclear configurations. When induced by light, these electronic and structural reorganizations can be extremely fast and coupled, as we recently reported for light-induced excited spin state trapping (LIESST).[1] Providing a relevant picture of the transformation process is necessary for developing light-activated functions. However, understanding electron-phonon coupling, conical intersection and energy redistribution is still a true challenge for both theoreticians and experimentalists, as these may occur beyond the Born–Oppenheimer approximation. This breakdown of the Born-Oppenheimer approximation is the basis of significant research interest in both fundamental and applied fields related to non-adiabatic phenomena. Their theoretical description requires treating coupled electron-nuclear dynamics by developing algorithms for time-propagation[2]. Obtaining an accurate multi-dimensional potential is challenging since it requires heavy calculations and potential energy surfaces are often limited to a small number of nuclear degrees of freedom. Several experimental tools developed during the last decades allow for probing, with femtosecond (fs) resolution, processes occurring at the time scale of nuclear motion or vibration in molecules, crystals and bio-systems. Femtochemistry, pioneered by A. H. Zewail,[3] demonstrated the power of fs optical pump-probe spectroscopy to describe chemical processes, probe in real-time electronic reorganization and molecular motions and monitor chemical reactions. This opened the way for developing various types of pump-probe techniques. To name a few, we can mention two-dimensional electronic spectroscopy,[4] able to probe quantum coherences and electronic couplings between different states, broadband impulsive vibrational spectroscopies[5], impulsive stimulated Raman[6] and also optical absorption[7], which are able to follow molecular vibrations during non-equilibrium dynamical processes. However, the fs optical pulses used in the IR, visible and ultraviolet regime deliver a very limited structural information. Therefore, femtosecond probes using electron pulses,[8] high harmonic generation[9] and X-ray[10] were developed. Compared to table-top plasma sources or synchrotron,[11] able to generate 100 fs X-ray pulses, X-FELs represent an ultimate source, generating much more intense X-ray pulses as short as few fs and with tunable wavelength.[12] A recent review detailed how time-resolved X-ray methods can map photoinduced electronic and structural dynamics of molecular systems.[13] These experimental inputs are very important for developing relevant theoretical models, with multi-dimensional potentials focussing on identified electronic states and key nuclear degrees of freedom. We will illustrate here how combined ultrafast optical and X-ray methods can deliver detailed view of the subtle and coupled changes of electronic and nuclear structures during molecular transformations, and provide a physical picture necessary for developing light-activated functions. Here we will focus our attention on transition metal complexes, which are of importance in biochemistry, catalysis, solar energy conversion, and photomagnetic materials for example. Understanding their light-activated processes, and the role of intermediate states, is crucial for the development of photochemistry and photophysics, especially systems based on iron, ruthenium, cobalt, copper, chromium or manganese. These prototypical systems show interdependent electronic and structural features that arise from the involvement of d orbitals in the valence configurations. Different competing false ground states, with different electronic and structural configurations may therefore exist.[14] Some of them may be reached at thermal equilibrium, but others may only appear under light excitation. Several recent studies highlighted the capabilities of X-ray techniques to deliver ultrafast changes of electronic state and structural dynamics, including coherent structural trapping, decoherence and incoherent motions. Hereafter we will introduce emerging techniques at X-FEL. For illustrating their capabilities, a large part of the paper is then focusing on the exciting developments in elucidation of the LIESST mechanism over the last 5 years. Finally, we mention other case studies broadening their range of application.

## 2. X-ray free electron lasers

X-FELs are linear accelerators, in which an electron bunch, travelling at essentially the speed of light, oscillates inside undulators. These linear magnetic structures, reaching 100 meter meters long, generate X-rays (Figure 1). The very same X-rays interact with the electrons in the bunch,[15] structuring the electron distribution.

[a] Prof Eric Collet, Dr Marco Cammarata
Univ Rennes, CNRS, IPR (Institut de Physique de Rennes) - UMR 6251, F-35000 Rennes, France
E-mail: eric.collet@univ-rennes1.fr

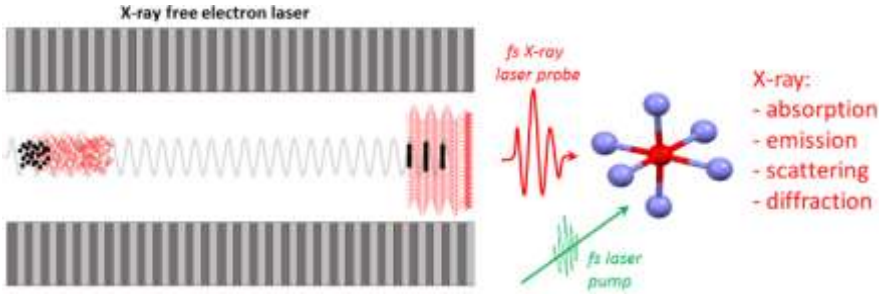


**Figure 1.** X-ray Free Electron Laser (X-FEL). Relativistic electrons (dots) propagating in an undulator, made of a periodic array of magnets (grey), emits X-rays (red). With self-amplified spontaneous emission, the emission of X-rays is correlated, ultrashort (1-100 fs) and very intense ($10^{12}$ photons per pulse). The fs X-ray laser pulse can be used for probing ultrafast molecular processes induced by a fs laser pump (green). A broad variety of X-ray techniques are applied in the time domain, such as absorption, emission, scattering or diffraction. They provide complementary information on electronic and structural dynamics involved during molecular transformations induced by light excitation.

This microbunching enhances the coherence and emittance of the radiation. The resulting self-amplified spontaneous emission (SASE) delivers hard X-ray pulses with up to $10^{12}$ photons per pulse on the sample and the X-ray pulse duration can reach 10 fs or less. This was demonstrated for the first time in the hard X-ray range at the Linac Coherent Light Source (LCLS) at SLAC (Stanford, USA)[16] and later at SACLA (Sayo, Japan).[17] More recently, the SwissFEL at the Paul Scherrer Institute (Villigen, Switzerland), the European X-FEL (Hamburg, Germany) and the PalFEL (Pohang, South Korea) came into play and delivered their first X-ray beams. Various pump / X-ray probe techniques are developed on the fs timescale on these X-FELs (Figure 1), including X-ray diffraction and scattering, absorption and emission spectroscopies.[13]

X-ray scattering experiments are performed on molecules in solution or in gas phase. The X-ray wave with an incident wave vector $k_i$, is scattered towards a new wave vector $k_s$ by the different atoms forming a molecule ($Q=k_s-k_i$). Interferences appear as each atom scatters the wave with an amplitude depending or the numbers of electrons and a phase depending on its relative position. By measuring I($Q$), the intensity dependence of the scattered wave with the momentum transfer between the incident and scattered wave vectors, the molecular structure can be found. X-ray diffraction experiments are performed on single crystal or powder. Because of the periodic 3D packing of atoms and molecules in real space, X-rays are diffracted into specific directions forming the nodes of the reciprocal space. A 3D picture of the mean positions of the atoms and of the electronic density in the crystal is determined from the intensities of these diffracted beams on the different Bragg peaks. These experiments provide key information on periodicity, symmetry, chemical bonds, crystallographic order and disorder, and many other information. Time-resolved X-ray scattering and diffraction techniques allows then for observing how structural parameters evolves in real-time.[11]

X-ray absorption spectroscopy (XAS) is widely used in the gas-phase, solution, or in solids.[18] This element-specific technique allows determining the local geometric and/or electronic structure around an absorbing atom. It consists in analysing how X-ray absorption changes with photon energy, as core electrons are

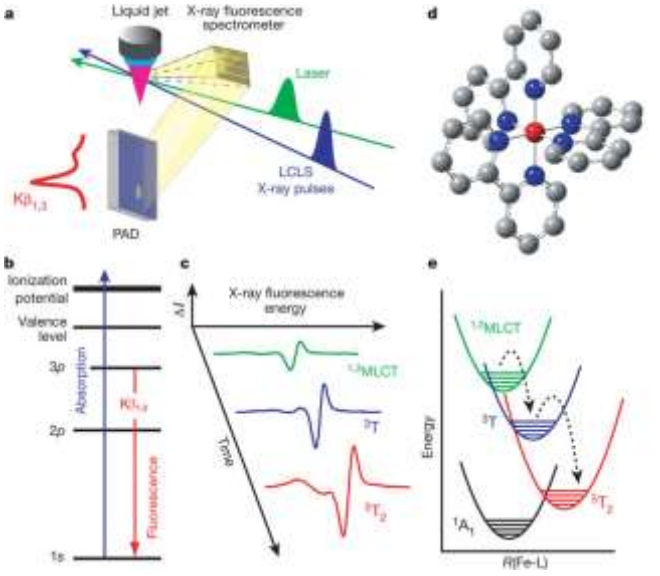


**Figure 2.** Schematic depiction of ultrafast X-ray fluorescence detection of LIESST. (a) Experimental set-up involving liquid jet for sample replenishment, optical laser pump, and 8-keV X-ray beam for generating X-ray fluorescence measured with a dispersive crystal spectrometer. (b) Energy level diagram for Kβ fluorescence involving photo-ionization of a 1s electron and X-ray fluorescence originating from the transition of a 3p electron to the 1s hole. (c) Schematic spectral dynamics. (d) Molecular structure of $[Fe(bpy)_3]^{2+}$. (e) schematic drawing of the dynamics on the potential energy surfaces. Reprinted with permission from Nature[19].

excited: 1s electron at the K-edge (Fig. 2b), 2s or 2p electron at the L-edge...[13] X-ray Absorption Near-Edge Structure (XANES) spectroscopy probes transitions from atomic core orbitals to valence orbitals, or to the continuum. The pre-edge transitions contain information about the occupancy of valence orbitals, involved in chemical bonding and chemical transformations. In the XANES region, the atom is ionized and the photoelectrons, with low kinetic energy, have high scattering cross-section. Their multiple scattering modulates the absorption, which contains information about the structure surrounding the absorbing atom. Well above the edge, the scattering of the ejected photoelectron by neighbouring atoms is mainly a single scattering event, responsible for the Extended X-ray Absorption Fine Structure (EXAFS).

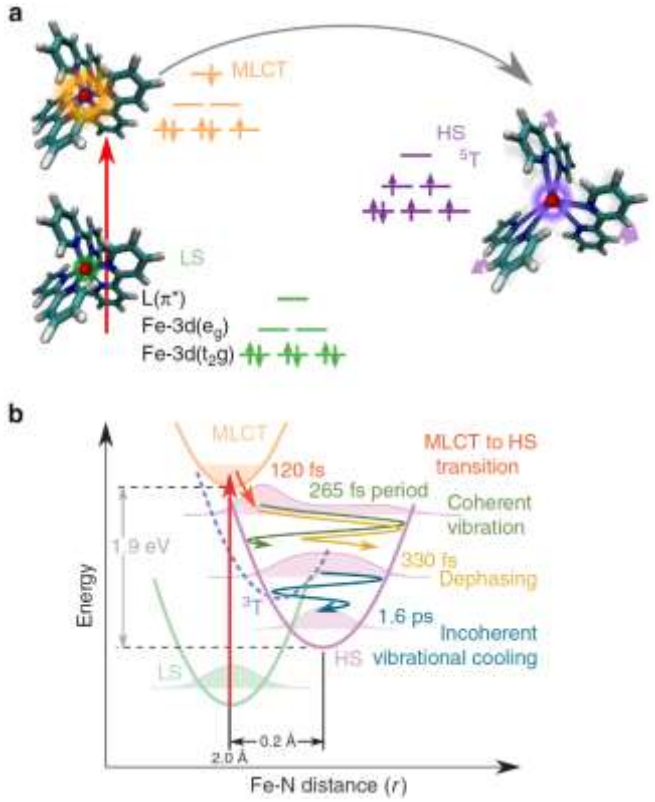


**Figure 3.** Schematic LIESST process. For the $[Fe(bpy)_3]^{2+}$ system, the Fe (red) is bonded to six N (blue) of the bpy ligands (L). After the initial photoexcitation of the LS state into an MLCT state (530 nm), the system decays towards the HS. The process and potential energy curves are represented along the Fe–N distance *r*, which is the structural coordinate. The ultrafast Fe-N elongation is rapidly trapping the system in the HS potential, where the system oscillates coherently (breathing mode, 265 fs period). The experiment was performed at room temperature in solution. Reprinted with permission from [1b].

It contains information about coordination numbers and bond distances to the nearest neighbours. In addition to X-ray absorption, X-ray emission spectroscopy (XES) provides additional information. For non-resonant XES, the absorption of a core electron and the transitions provide strong sensitivity to the chemical environment of the emitting atom (ligand orbitals, bond distances). Resonant X-ray emission spectroscopy allows probing the occupied and unoccupied density of states around the resonant core excitation through the resolution of both the incident and emitted photon energies. We will illustrate hereafter how such ultrafast techniques open the way for disentangling electronic and structural dynamics during ultrafast molecular transformations.

## 3. Light-induced excited spin-state trapping

When a transition metal ion is surrounded by ligands in close proximity, the d orbitals split in low energy and high energy levels (pointing between and towards the ligands respectively). Electron-electron repulsion and the energy gap between these two groups of orbitals usually result in different electronic configurations with different number of paired electrons, i.e. to different spin states. The ability of transition metal complexes to change between low (LS) to high (HS) spin states at thermal equilibrium (under the effect of temperature or pressure) or out-of-equilibrium by light irradiation has attracted much interest in chemistry, physics and material science. Molecular transformations involving drastic changes of spin state ($\Delta S=2$) are interesting in material science for applications in magnetic data storage/optical reading due to photomagnetic and photochromic properties for example.[20] They are also of direct relevance to biology,[21] since for example the active site of hemoproteins are made of complexed Fe(II) or Co(II). A diagram of the potential energy curves of close-to-octahedral Fe(II)-based complexes, connected with the various bonding nature of the different electronic states, is shown in Figure 3. The potential energy curves are represented along the Fe-N bond length, which is the main structural change, as shown by structural studies in the solid state[22] and in solution.[1b] The ground state is $^1A_1$ (LS, S=0) with an electronic distribution $t_{2g}^6e_g^0L^0$, where L refers to unoccupied ligand orbitals. The HS state is $^5T_2$ (S=2, $t_{2g}^4e_g^2L^0$) and because the $e_g$ orbitals are antibonding in 6-fold coordinated complexes, a striking elongation of the metal-ligand bond occurs in the HS state. Many $Fe^{2+}$, $Fe^{3+}$, $Mn^{3+}$ and $Co^{2+}$ spin crossover complexes (SCO) were synthesized and investigated, as some of them undergo Light-Induced Excited Spin-State Trapping (LIESST).[23] From the beginning it was understood that light excitation into the Metal-to-Ligand-Charge-Transfer ($^1$MLCT) state, or into lower-lying ligand field states, leads to the population of the lowest quintet HS state $^5T_2$ with unity quantum yield.[23-24] Structural studies performed by X-ray diffraction or absorption at low temperature, where the photoinduced HS state is long-lived, evidenced the ~0.2 Å elongation of the Fe-N bond for Fe(II)-based complexes, which is similar to the one observed during the thermal conversion from LS to HS.[25] But the dynamics of the process and the role of the structural reorganization were questioned.[26] Various pump-probe studies were performed on spin-crossover materials and mainly with $Fe^{II}N_6$ ligand field core under MLCT excitation in the ≈1-3 eV range. These revealed that LIESST is ultrafast (≈200 fs) at the molecular level and occurs on similar timescales in solution and in crystal, from 100 to 300K.[1b, 7a, 10, 19, 27] More recently, the reverse-LIESST (HS to LS) process was found to be slower (ps timescale) and better described in a kinetic way.[28] In solids, the molecular expansion related to LIESST induces, through the elastic interaction between the molecules, a global lattice dilation related to macroscopic transformation. A recent work made use of this light-induced molecular expansion to demonstrate that the internal pressure within the lattice induced by LIESST can drive cooperative transformation: a single photon can transform more than 7 molecules.[29] The process driving the important reorganizations of electronic and structural degrees of freedom, the sequence of intermediates and the nature of the vibrations observed by time-resolved studies during LIESST were subjects of intense discussions. Indeed, the interpretation of optical data is rather indirect in terms of electronic state or structural change and some spin states are optically silent.

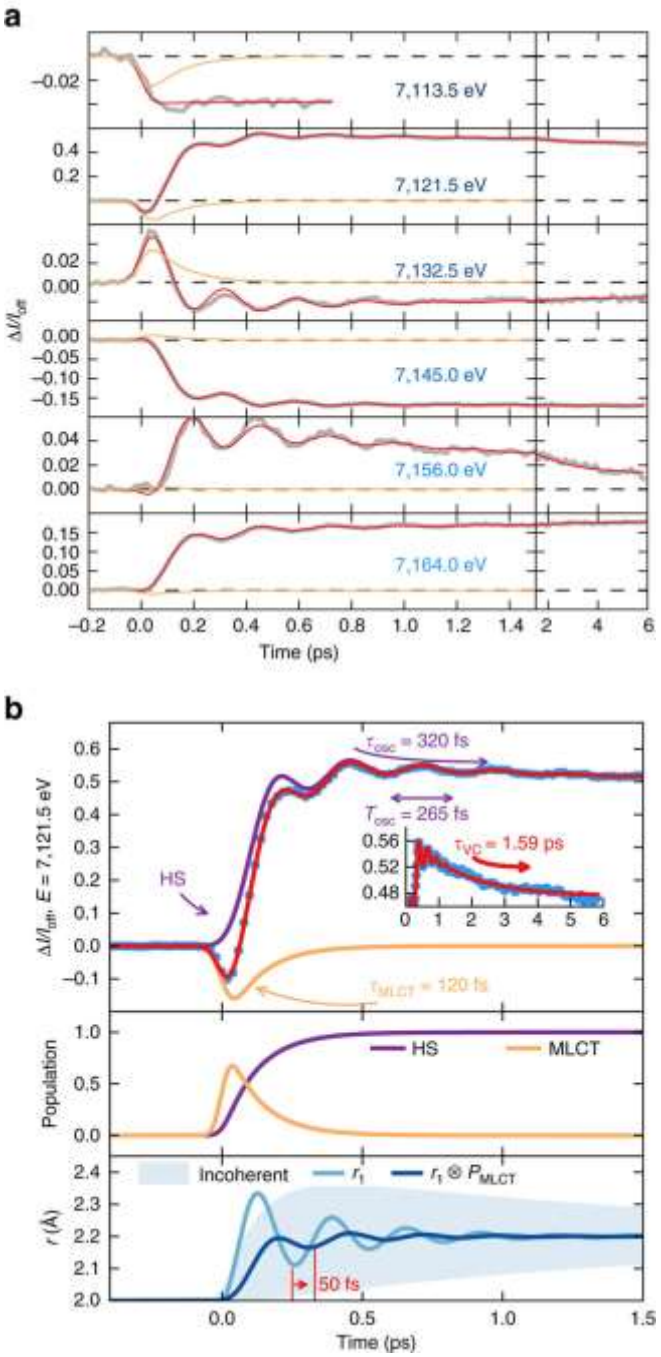


**Figure 4.** (a) Time scans of relative absorption change at selected X-ray energies (solid grey lines) revealing 126(3) $cm^{-1}$ oscillations. Red lines correspond to the fit of the data set. The dynamic parameters are the same for all energies: MLCT lifetime $\tau_{MLCT}$=120(10) fs, oscillation period $T_{OSC}$=265(10) fs and damping $\tau_{OSC}$=320(10) fs and vibrational cooling $\tau_{VC}$=1.6(0.1) ps. Orange lines represent the MLCT contributions. (b) Example fit for 7121.5 eV (top panel), showing the individual contributions of MLCT and oscillating HS contributions along with the total signal. The model disentangles the electronic kinetic description (MLCT and HS population, mid panel) from the structural dynamics given by the time evolution of the average Fe–N distance *r* (bottom). The exponential growth of the HS population from the MLCT leads to an average coherent oscillating trajectory (dark blue), which has a reduced amplitude and apparent phase shift (≈50 fs) with respect to a directly initiated damped oscillating trajectory $r_1(t)$ in the HS potential. The incoherent part of the oscillations, decays within 1.6 ps. Reprinted with permission from NPG[1b].

On the one hand, Gawelda et al.[30] used hard X-ray pulses at the K edge of Iron for probing with 70 ps resolution the structure of the HS state induced by laser excitation. This high quality data measurement of photoexcited $[Fe^{II}(bpy)_3]^{2+}$ was however lacking time resolution for understanding the dynamics of the process. On the other hand, Bressler et al.[10] used the slicing technique at the SLS synchrotron for tracking XANES changes with ≈200 fs resolution[31]. They evidenced that Fe-N bonds elongate within 150±50 fs as the HS state is reached, but the low X-ray flux of this techniques limited the investigations. Huse et al. used fs soft X-ray spectroscopy for deciphering the interplay of electronic and structural dynamics during the LIESST process of $[Fe(tren(py)_3)]^{2+}$ and found a time constant of 85(75) fs for the formation time of the HS state.[32] The most recent LIESST studies in Fe(II) systems, performed at X-FEL, illustrate perfectly the new possibilities offered by X-ray lasers as the intense X-ray flux and the high time resolution can provide detailed information on changes of electronic and nuclear configurations during the intersystem crossing (ISC). Ultrafast X-ray spectroscopies provide key information on the electronic and structural changes,[1b, 22, 27a] whereas X-ray scattering of molecules in solution[33], or X-ray diffraction[34] in crystals, provide more global information on the structural dynamics. Gaffney et al. performed fs X-ray emission spectroscopic (XES) on photoexcited $[Fe^{II}(bpy)_3]^{2+}$ at LCLS.[19] The time-resolved $K_\beta$ fluorescence spectra, sensitive to spin state, allowed monitoring the time course of the electronic configuration rearrangement. In this way, they evidenced a short passage via the $^3T$ state (Figure 2), from the MLCT to the HS state. Their kinetic modelling allowed distinguishing the $^{1,3}$MLCT electronic excited state, the intermediate $^3T$ state and the final $^5T_2$ HS state in the relaxation cascade. The experimental time resolution (~125 fs) limited the description of the dynamics, but provided a ≈120 fs timescale for the MLCT→ $^3T$ conversion and ≈70 fs for the $^3T$→HS conversion. This picture has been debated based on high time-resolution optical experiments, which suggested that the HS state is impulsively populated in less than 50 fs.[7a]

As XES experiments lack direct structural information, Lemke et al. used XANES at the LCLS X-FEL for tracking, with high signal-to-noise signal and 25 fs root-mean-square resolution, electronic and structural dynamics of photoexcited $[Fe^{II}(bpy)_3]^{2+}$.[1b] The transient XANES intensity changes $\Delta I(t)/I_{off}$ after photoexcitation (Figure 4a) were measured at different X-ray energies. In the pre-edge region (7113.5 eV), the absorption decreases in the HS state, compared to LS state, as $e_g$ states become occupied. Well above the edge (7164 eV) $\Delta I(t)/I_{off}$ is predominantly sensitive to the Fe-N elongation, whereas intermediate energies are sensitive to both electronic and structural reorganizations. The change of signal sign at around 100 fs for some time traces evidences clearly a short-lived intermediate electronic state. The data analysis evidenced that the initial photoinduced state is the MLCT as the amplitudes of XANES changes correspond to a formal $Fe^{3+}$ electronic state ($t_{2g}^4 e_g^1 L^1$), characterized by ≈1 eV shift of the XANES spectrum compared to the LS $Fe^{2+}$ spectrum. Those traces also show damped oscillations.

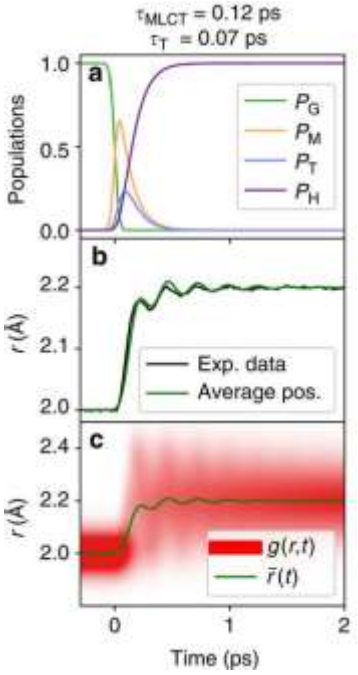


**Figure 5.** Simulations of the transient molecular distribution in coordinate *r* for MLCT→HS ($\tau_{MLCT}$=120 fs) and MLCT→3T→HS ($\tau_T$=70 fs) electronic state transition (a–c,d–f, respectively). The time-dependent populations of the different electronic states are shown in panels (a and d), which give rise to the calculated distribution g(r,t) and average coordinate *r*: $\bar{r}(t)$ (c,f). The experimental data at 7145 eV (blue) scaled in *r* has additionally been overlaid with the simulated signal (b,e). Reprinted with permission from NPG [1b].

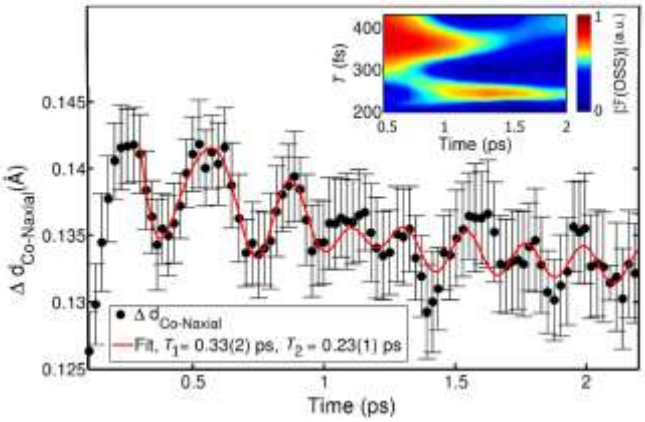


**Figure 6.** Time evolution of the Co–N bond lengths (black dots) of photoexcited $[Co^{II}(bpy)_3]^{2+}$, retrieved from the fs X-ray scattering data. The insert shows a time-resolved Fourier transform of the oscillatory part of the difference scattering signal indicating sequential activation of two vibrational modes. The red line shows a heuristic fit, incorporating sequential activation of first a $T_1 \sim 0.33$ ps mode and then a $T_2 \sim 0.23$ ps mode identified as, respectively, breathing- and pincer-like by direct comparison with our DFT calculations. Reprinted with permission from reference [33]. Copyright 2018 American Physical Society.

The data analysis included the MLCT decays within 120 fs, the 70 fs passage through the $^3$T (Figure 5) and the stochastic population of the HS state. The time evolution of the electronic state was then decoupled from the structural dynamics (Fig. 4b), described in terms of the temporal evolution of *r*, which is the average bond length between the Fe and the six N atoms of the bpy ligand. *r(t)* was extracted from the data through XANES multiple scattering calculations of the molecular structure, as at 7145 eV the signal changes linearly with *r*. This is naturally connected to the totally symmetric elongation of the 6 Fe-N bonds from 2.0 to 2.2 Å between LS and HS states, which is the main reaction coordinate in terms of structural change (Fig. 3). After the fast ISC from MLCT to HS, the antibonding $e_g$ orbitals are populated. The equilibrium position of the potential energy curves shifts then towards longer Fe-N bonds (*r*) and the mechanism is therefore displacive along *r*. It induces coherent and cosine types oscillatory motions in the HS potential (Fig. 4b). The observed vibration at 126 $cm^{-1}$, also found to modulate transient optical absorption data,[7a] was unambiguously assigned to the $a_{1g}$ breathing mode of $[Fe^{II}(bpy)_3]^{2+}$ in the HS state.[1b] It corresponds to the in-phase stretching of the 6 Fe-N bonds, and therefore of *r(t)*, with almost rigid ligands. As explained by Lemke et al.,[1b] the exponential growth of the HS population from the MLCT leads to an average coherent oscillating trajectory $\overline{r(t)} = r_1(t) \otimes P_{MLCT}(t)$ with reduced amplitude and apparent phase shift (≈50 fs) with respect to a directly initiated damped oscillating trajectory $r_1(t)$ in the HS potential (Fig. 4b). Similar oscillations were observed with femtosecond X-ray scattering at the LCLS X-FEL by Biasin et al.[33] (Figure 6) on photoexcited $[Co^{II}(terpy)_2]^{2+}$. The $Co^{II}$ $d^7$ electronic configuration can be either a LS doublet state or a HS quartet state and the transformation pathway does not involve intermediate spin state. This technique, directly sensitive to the global structural changes, evidenced the ultrafast elongation and oscillation of the Co–N bonds during LIESST, followed by another coherent Co–N bond length oscillations. These totally symmetric stretching modes of $[Co^{II}(terpy)_2]^{2+}$ are similar to the breathing mode observed of $[Fe^{II}(bpy)_3]^{2+}$.

Both X-ray absorption spectroscopy and X-ray scattering experiments found that the amplitude of the oscillation of the average $\bar{r}$ (Figure 4) is significantly smaller than the ≈ 0.2 Å bond elongation observed during the LS to HS conversion. This structural decoherence or dephasing of the initially excited wave packet is related to the ISC timescale: the overall ≈150 fs time conversion from MLCT to HS potential is relatively long, compared to the period of the breathing mode. Indeed, it approaches the limit for maintaining structural coherence, as the ISC timescale is close to the ≈130 fs ½ period of the mode. The dephasing along *r* can be qualitatively monitored by the X-ray absorption at energies where absorption change nonlinearly with *r* (Figure 4). It is the case at 7156 eV for $[Fe^{II}(bpy)_3]^{2+}$, where X-ray absorption is minimum in the HS state for *r*=2.2 Å, *i.e.* the equilibrium structure.[1b] Bonds shorter or longer than 2.2 Å contribute to an increase of X-ray absorption. A quantitative degree of delocalization was obtained by using DFT calculations and a model describing the activation and dephasing of the breathing mode to analyse the data, through the evolution of *g(r,t)*, which is the distribution of *r*.[1b] The degree of delocalization along *r* (Figure 5) is large after the ISC and it gets sharper within $\tau_{VC}$ =1.6 ps, as vibrational cooling occurs in the HS potential.

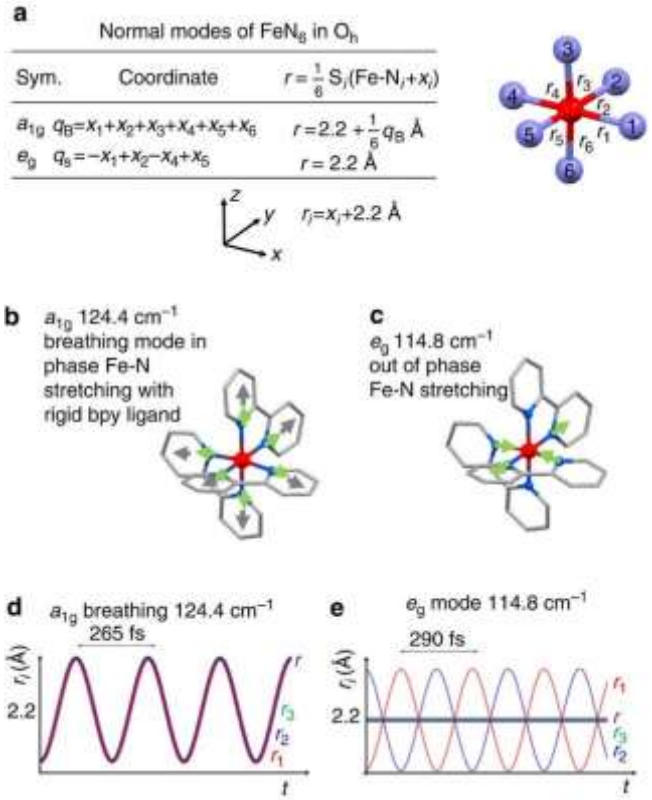


**Figure 7.** Representation of some HS normal modes obtained from DFT calculation: (a) Fe-N bond coordinate and average length $r$ for $a_{1g}$ and $e_g$ symmetry normal modes, (b) $a_{1g}$ breathing mode (124.4 $cm^{-1}$, in-phase stretching of the 6 Fe-$N_i$ bonds with almost rigid bpy ligands), (c) $e_g$ stretching modes at 114.8 $cm^{-1}$. Green arrows show N motions and grey ones ring motions. (d,e) Time evolution of the symmetry independent bonds (with respect to the inversion symmetry) $r_1$, $r_2$ and $r_3$ and their average $r$ (purple) for the $a_{1g}$ and $e_g$ modes. Modified from [1b].

This initial dispersion in $r$ is not only related to the dispersion of the reaction coordinate $r$ due to the dephasing of the breathing mode. Indeed, it is also important to consider that other modes are activated during the process, and that their symmetry may allow coherent or incoherent activation during the ISC. The breathing mode $q_B$, is totally symmetric ($a_{1g}$ for $O_h$ point group, Figure 7a,b), as the six Fe-$N_i$ bond lengths $r_i$ oscillate in phase by $x_i$ around $r$≈2.2 Å. $q_B$ transforms like $r$ and $r(t)$= <$r_i(t)$>. During the ISC from MLCT to HS potentials, the equilibrium value of $r$ elongates from 2.0 to 2.2 Å. This ISC launches therefore the $q_B$ mode and $q_B(t)$ and $r(t)$, undergo cosine damped oscillation, with a maximum amplitude at t=0 when the ISC starts (Figure 7). As this process occurs on a timescale shorter than the half period of the mode, all the photoexcited molecules oscillate almost in phase and coherent oscillations related to fast ISC can be observed. The fast damping of the molecular breathing is an important feature explaining the high quantum efficiency of LIESST. Veenendaal et al. underlined the role of the energy dissipation towards other modes, which destroys the coherence and the amplitude of the breathing mode, therefore precluding recurrence towards the initial LS state.[26] This energy redistribution during the process can activate incoherently different modes, and this process can also broaden the Fe-N distribution around its equilibrium value. Indeed, in addition to the Fe-N broadening due to activation and decoherence along $q_B$ during the ISC, lower symmetry modes also play their role. This is the case for example of the $e_g$ Fe-N stretching vibration $q_S$, which keep $r$ constant in time, as shown in Figs 7c,e. As the ISC is isostructural (without symmetry change) the equilibrium positions correspond to $q_S$=0 in both LS ($r$=2.0 Å) and HS ($r$=2.2 Å) potential energy surfaces, represented along the $q_B$ and $q_S$ coordinates in Figure 8. When energy is redistributed during the ISC, vibrations like $q_S$ act as a thermal bath and contribute to vibrational cooling. The ps timescale of the energy deposition on these modes is long compared to their period and such low symmetry modes are equally launched along $+q_s$ or $-q_s$. Therefore, modes like $q_S$ are incoherently activated (with no phase origin) and contribute to the broadening of the distribution of $r$ (Figure 7e). The distribution along $q_S$ (Fig. 8) therefore broadens during the ISC and narrows as the bottom of the HS potential is reached during the vibrational cooling, whereas $q_B$ undergoes damped coherent oscillation. The time-dependent XANES signal at 7156 eV (Figure 4), which decays with a 1.6 ps constant, constitutes then a direct observation of the vibrational cooling process, observed here by selectively probing the narrowing of the molecular distribution along the reaction coordinate $r$, as schematically represented in Figure 3.

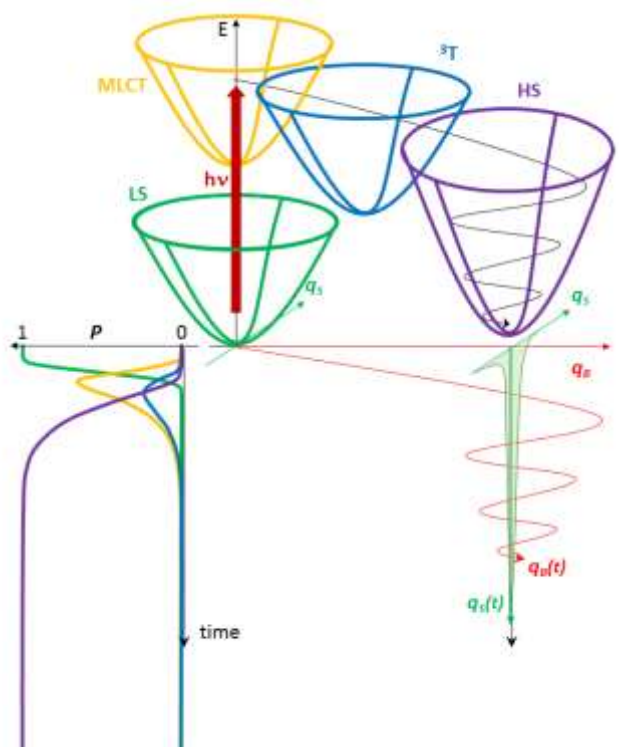


**Figure 8.** Conceptual description of LIESST, made possible with fs X-FEL studies. The population $P$ of the different electronic states during ISC (color code) is monitored by XANES or XES studies, whereas XANES, X-ray diffraction or scattering can probe structural changes along the breathing reaction coordinate $q_B$. It is also possible to discriminate the coherent structural dynamics along the breathing reaction coordinate $q_B$ from the incoherent dynamics along lower symmetry modes ($q_S$).

These advances in ultrafast X-ray science provide more and more detailed studies, allowing decoupling in real time electronic and structural dynamics during ISC, as schematically shown in Figure 8 for LIESST. The populations of the different electronic states, obtained from XES and/or XANES, are decoupled from the coherent or incoherent structural dynamics obtained from XANES or scattering. By identifying a limited but relevant number of electronic states and structural vibration modes, X-FEL can also help developing relevant theoretical models. Recent calculations used time-dependent approaches to provide intersystem-crossing rates during LIESST in agreement with these experimental reports,[35] or to underline the role of the breathing mode in the processes.[26] However, the coupled coherent and incoherent structural dynamics and the energy redistribution process accompanying ISC and trapping the system are still poorly understood or described in the literature.

## 4. Exploring different photoswitching pathways

The results discussed above underline the importance of the ISC timescale for the structural decoherence along the reaction coordinate (such as Fe-N elongation for LIESST). This is because the LS and MLCT states are equally bonding (as their antibonding $e_g$ orbitals are not populated). Indeed, the structural elongation starts only when the $^3$T state is reached, and this process is driven by the electron-phonon coupling. Faster elongation and larger structural coherence is therefore expected in the case of a direct excitation towards $e_g$ states, for bypassing the MLCT→$^3$T ISC. However, LIESST was mainly investigated in $FeN_6$ systems of almost octahedral symmetry, precluding a direct population from $t_{2g}$ to $e_g$ like orbitals (dipole moment is an odd operator and d orbitals are even). We investigated, by using fs pump-probe spectroscopy, LIESST in the $Fe^{II}(pap\text{-}5NO_2)_2$ system, which has an $FeN_4O_2$ ligand field of $C_2$ symmetry. We compared the response of the allowed d-d "$t_{2g}$→$e_g$ like" excitation at 730 nm to the MLCT photo-excitations at 530 nm [7b] (Figure 9). We found that under MLCT excitation, the 120 fs MLCT→T ISC and the 70 fs T→HS ISC are very similar to the ones reported for $FeN_6$ systems and these ISC. The process is also accompanied by the fast activation and damping of the molecular breathing mode. DFT calculation revealed the breathing nature of this mode, whereas TD-DFT calculations explained why it modulates optical absorption, especially around the d-d optical gap,[7b] as also reported in the $[Fe(phen)_2(NCS)_2]$ system.[36] Here again, the coherent structural dynamics moves the system between different electronic potentials, on a timescale where wave functions of atomic nuclei and electrons are difficult to separate. If the timescale of the structural trapping through Fe-Ligand elongation is limited by the decay of the MLCT towards the T state, under d-d excitation the instantaneous population of antibonding orbitals launches immediately the Fe-Ligand expansion towards the HS potential, which is reached within 70 fs. This d-d excitation pathway limits the structural decoherence and increases the amplitude of the oscillations (Figure 9).

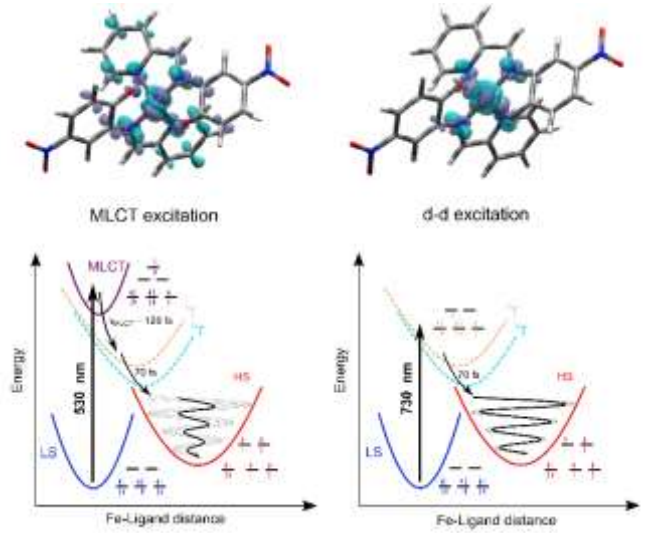


**Figure 9.** LIESST under MLCT (530 nm, left) and d-d (730 nm, right) excitation. The electronic decays towards less bonding $^3$T and HS states increases the equilibrium Fe-Ligand distance and launches coherent Fe-L breathing. The amplitude of the coherent oscillation is larger under d-d than MLCT excitation because the HS potential is reached more rapidly. Reprinted with permission from[7b].

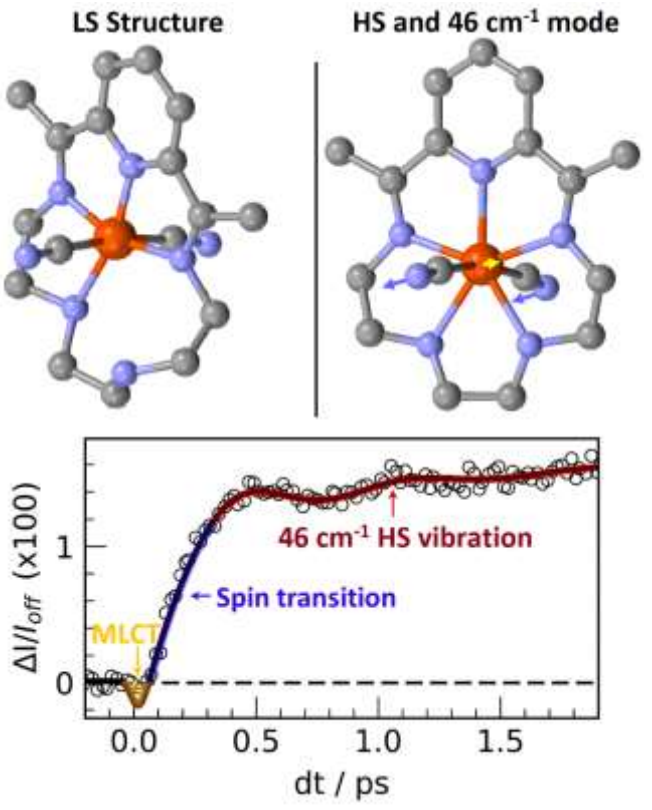


**Figure 10.** LIESST in $[Fe^{II}(L_{222}N_5)(CN)_2]$, with LS and HS structures, and representation of the 46 cm$^{-1}$ mode related to the NC-Fe-CN bending. The fit of the time resolved change of the relative X-ray absorption $\Delta I(t)/I_{off}$ measured at 7125 eV takes into account the spin transition with the MLCT to HS decay and a damped oscillation with 710 fs period (47 cm$^{-1}$). Modified from reference [1a]

A similar study, both under MLCT and d-d like photoexcitations, concerned the low symmetry $[Fe^{II}(L_{222}N_5)(CN)_2]$ coordination compound (Figure 10).[1a] Optical and X-ray spectroscopies gave ISC timescales similar to those discussed above (≈120 fs for MLCT and 70 fs for d-d excitation respectively). But the structural description is more complex since the reorganization involves both changes of bond lengths, coordination and symmetry from the hexa- LS ($C_1$) to hepta-coordinated HS ($C_{2v}$) states. Several degrees of freedom can therefore play their role, making the PES more complex to describe and challenging to calculate. The high frequency breathing mode is then incoherently populated, whereas a slower mode at 46 $cm^{-1}$ (Figure 10, bending of the C-N groups) is found to be coherently activated.

## 5. Summary and outlook

The recent studies presented above, combining ultrafast X-ray absorption, emission, scattering or diffraction, illustrate the power of time-resolved techniques for understanding molecules at work. In addition to existing facilities at synchrotron or table-top HHG sources, lacking time resolution or X-ray flux, X-ray free electron laser make the best use of the fs time resolution and extremely high X-ray flux for studying light-induced molecular transformations. The use of shorter and shorter pulses of light and X-ray allows now for observing and enhancing coherence. This is of great importance for photoinduced phenomena, as a recent evidence of coherence in chemical and biological systems suggests that the phenomena can be used in complex chemical systems as a design element in realizing function.[37]

Among different case studies, CT processes are of interest for X-ray spectroscopies, which provide oxidation state of elements. It is now possible to track CT with femtosecond resolution, especially in the case of intersite CT, by studying changes at the edges of the departure and arrival elements. Canton et al.[38] combined fs XES and X-ray scattering (XRS) at the X-FEL SACLA to characterize the ultrafast electron transfer dynamics in a bimetallic complex. In this way, they could nail down the dynamics of electron departure from Ru-based chromophore, its transit time via the bridge connecting Ru to Co sites, its arrival to the Co, and the spin transition on the Co. This study exemplifies the wide class of synthetic and natural photocatalysts, which can be investigated by X-FEL based techniques. Another example in material science is the family of Prussian Blue Analogues, for which the ultrafast photoinduced CT between metallic sites is responsible for the appearance of magnetic properties. The preliminary XANES studies performed with 100 ps resolution[39] are nowadays performed with a time resolution shorter than 100 fs for investigating if the appearance of magnetism is a charge-transfer induced spin transition or a spin-transition-induced charge-transfer. X-ray spectroscopies extending now to softer regime will make it possible to probe spectral changes around the K-edge of light elements such as C, N, O, S... This is of great interest for exploring dynamics in many molecular systems, around these elements playing a central role in coordination chemistry, material science and in biology. Finally, the emerging serial femtosecond crystallography at X-FEL allows now reconstructing 3D structural reorganization, as illustrated by a recent study evidencing the sub-ps trans-to-cis isomerization of a chromophore.[40] It is very likely that this technique will be applied to study various photoinduced processes in crystals as it provides accurate measurements of atomic motions.

The door is now open to tackle more complex problems as X-ray free electron lasers broaden the range of methods that can be implemented to characterise molecular systems on femtosecond timescale. This will boost the capabilities to gather new insight into electronic and structural changes involved during light-induced phenomena for a better understanding and control of photoactivated molecular functions.

## Acknowledgements

We would like to thank H. Lemke, R. Bertoni and M. Lorenc our close collaborators in the field of ultrafast X-ray science. We thank the ANR (ANR-13-BS04-0002 FEMTOMAT and ANR-15-CE32-0004 Bio-XFEL) and Centre National de la Recherche Scientifique (CNRS) (PEPS SASLELX) for financial support.

**Keywords:** Ultrafast • Intersystem Crossing • XANES • XES • LIESST

[1] a) S. Zerdane, E. Collet, X. Dong, S. F. Matar, H. F. Wang, C. Desplanches, G. Chastanet, M. Chollet, J. M. Glownia, H. T. Lemke, M. Lorenc and M. Cammarata, *Chemistry* **2018**, *24*, 5064-5069; b) H. T. Lemke, K. S. Kjær, R. Hartsock, T. Brandt van Driel, M. Chollet, J. M. Glownia, S. Song, D. Zhu, E. Pace, S. F. Matar, M. N. Nielsen, M. Benfatto, K. J. Gaffney, E. Collet and M. Cammarata, *Nat. Commun.* **2017**, *8*, 15342.

[2] a) J. O. Richardson, P. Meyer, M.-O. Pleinert and M. Thoss, *Chemical Physics* **2017**, *482*, 124-134; b) B. F. E. Curchod, U. Rothlisberger and I. Tavernelli, *Chemphyschem* **2013**, *14*, 1314-1340.

[3] A. H. Zewail, *Angewandte Chemie-International Edition* **2000**, *39*, 2587-2631.

[4] A. Halpin, P. J. M. Johnson, R. Tempelaar, R. S. Murphy, J. Knoester, T. L. C. Jansen and R. J. D. Miller, *Nature Chemistry* **2014**, *6*, 196.

[5] M. Liebel, C. Schnedermann, T. Wende and P. Kukura, *J Phys Chem A* **2015**, *119*, 9506-9517.

[6] D. R. Dietze and R. A. Mathies, *Chemphyschem* **2016**, *17*, 1224-1251.

[7] a) G. Aubock and M. Chergui, *Nature Chemistry* **2015**, *7*, 629-633; b) S. Zerdane, L. Wilbraham, M. Cammarata, O. Iasco, E. Rivière, M. L. Boillot, I. Ciofini and E. Collet, *Chem. Sci.* **2017**, *8*, 4978-4986.

[8] a) M. Dantus, S. B. Kim, J. C. Williamson and A. H. Zewail, *Journal of Physical Chemistry* **1994**, *98*, 2782-2796; b) Y. Jiang, L. C. Liu, H. M. Müller-Werkmeister, C. Lu, D. Zhang, R. L. Field, A. Sarracini, G. Moriena, E. Collet and R. J. D. Miller, *Angewandte Chemie International Edition* **2017**, *56*, 7130-7134.

[9] a) A. R. Attar, A. Bhattacherjee, C. D. Pemmaraju, K. Schnorr, K. D. Closser, D. Prendergast and S. R. Leone, *Science* **2017**, *356*, 54-59; b) Z. Chang, *Frontiers in Optics 2017* (Washington, D.C.) **2017**, p. LTu4F.1; c) Y. Pertot, C. Schmidt, M. Matthews, A. Chauvet, M. Huppert, V. Svoboda, A. von Conta, A. Tehlar, D. Baykusheva, J.-P. Wolf and H. J. Wörner, *Science* **2017**, *355*, 264-267; d) J. Vura-Weis, C. M. Jiang, C. Liu, H. W. Gao, J. M. Lucas, F. M. F. de Groot, P. D. Yang, A. P. Alivisatos and S. R. Leone, *Journal of Physical Chemistry Letters* **2013**, *4*, 3667-3671.

[10] C. Bressler, C. Milne, V. T. Pham, A. ElNahhas, R. M. van der Veen, W. Gawelda, S. Johnson, P. Beaud, D. Grolimund, M. Kaiser, C. N. Borca, G. Ingold, R. Abela and M. Chergui, *Science* **2009**, *323*, 489-492.

[11] E. Collet, *Acta Crystallographica Section A* **2010**, *66*, 133-134.

[12] C. Bostedt, S. Boutet, D. M. Fritz, Z. Huang, H. J. Lee, H. T. Lemke, A. Robert, W. F. Schlotter, J. J. Turner and G. J. Williams, *Reviews of Modern Physics* **2016**, *88*, 015007.
[13] M. Chergui and E. Collet, *Chemical Reviews* **2017**, *117*, 11025–11065.
[14] K. Nasu, H. Ping and H. Mizouchi, *J. Phys.: Condens. Matter* **2001**, *13*, R693.
[15] G. Margaritondo and P. Rebernik Ribic, *J Synchrotron Radiat* **2011**, *18*, 101-108.
[16] P. Emma, R. Akre, J. Arthur, R. Bionta, C. Bostedt, J. Bozek, A. Brachmann, P. Bucksbaum, R. Coffee, F. J. Decker, Y. Ding, D. Dowell, S. Edstrom, A. Fisher, J. Frisch, S. Gilevich, J. Hastings, G. Hays, P. Hering, Z. Huang, R. Iverson, H. Loos, M. Messerschmidt, A. Miahnahri, S. Moeller, H. D. Nuhn, G. Pile, D. Ratner, J. Rzepiela, D. Schultz, T. Smith, P. Stefan, H. Tompkins, J. Turner, J. Welch, W. White, J. Wu, G. Yocky and J. Galayda, *Nature Photonics* **2010**, *4*, 641-647.
[17] T. Ishikawa, H. Aoyagi, T. Asaka, Y. Asano, N. Azumi, T. Bizen, H. Ego, K. Fukami, T. Fukui, Y. Furukawa, S. Goto, H. Hanaki, T. Hara, T. Hasegawa, T. Hatsui, A. Higashiya, T. Hirono, N. Hosoda, M. Ishii, T. Inagaki, Y. Inubushi, T. Itoga, Y. Joti, M. Kago, T. Kameshima, H. Kimura, Y. Kirihara, A. Kiyomichi, T. Kobayashi, C. Kondo, T. Kudo, H. Maesaka, X. M. Marechal, T. Masuda, S. Matsubara, T. Matsumoto, T. Matsushita, S. Matsui, M. Nagasono, N. Nariyama, H. Ohashi, T. Ohata, T. Ohshima, S. Ono, Y. Otake, C. Saji, T. Sakurai, T. Sato, K. Sawada, T. Seike, K. Shirasawa, T. Sugimoto, S. Suzuki, S. Takahashi, H. Takebe, K. Takeshita, K. Tamasaku, H. Tanaka, R. Tanaka, T. Tanaka, T. Togashi, K. Togawa, A. Tokuhisa, H. Tomizawa, K. Tono, S. K. Wu, M. Yabashi, M. Yamaga, A. Yamashita, K. Yanagida, C. Zhang, T. Shintake, H. Kitamura and N. Kumagai, *Nature Photonics* **2012**, *6*, 540-544.
[18] M. Chergui, *Structural Dynamics* **2016**, *3*, 031001.
[19] W. K. Zhang, R. Alonso-Mori, U. Bergmann, C. Bressler, M. Chollet, A. Galler, W. Gawelda, R. G. Hadt, R. W. Hartsock, T. Kroll, K. S. Kjaer, K. Kubicek, H. T. Lemke, H. Y. W. Liang, D. A. Meyer, M. M. Nielsen, C. Purser, J. S. Robinson, E. I. Solomon, Z. Sun, D. Sokaras, T. B. van Driel, G. Vanko, T. C. Weng, D. L. Zhu and K. J. Gaffney, *Nature* **2014**, *509*, 345-348.
[20] M. A. Halcrow, *Spin-crossover materials : properties and applications*, Wiley, **2013**, p. xviii, 546 p.
[21] M. Levantino, H. T. Lemke, G. Schirò, M. Glownia, A. Cupane and M. Cammarata, *Structural Dynamics* **2015**, *2*, 041713.
[22] M. Cammarata, R. Bertoni, M. Lorenc, H. Cailleau, S. Di Matteo, C. Mauriac, S. F. Matar, H. Lemke, M. Chollet, S. Ravy, C. Laulhe, J. F. Letard and E. Collet, *Physical Review Letters* **2014**, *113*, 227402.
[23] a) S. Decurtins, P. Gutlich, K. M. Hasselbach, A. Hauser and H. Spiering, *Inorganic Chemistry* **1985**, *24*, 2174-2178; b) A. Hauser, *Spin Crossover in Transition Metal Compounds Ii* **2004**, *234*, 155-198; c) H. A. Goodwin, *Spin Crossover in Transition Metal Compounds Ii* **2004**, *234*, 23-47.
[24] S. Decurtins, G. P., K. C.P. and H. Spiering, *Chemical Physics Letters* **1984**, *105*, 4.
[25] E. Collet and P. Guionneau, *Comptes Rendus Chimie* **2018**.
[26] M. van Veenendaal, J. Chang and A. J. Fedro, *Physical Review Letters* **2010**, *104*, 067401.
[27] a) A. Marino, M. Cammarata, S. F. Matar, J.-F. Létard, G. Chastanet, M. Chollet, J. M. Glownia, H. T. Lemke and E. Collet, *Structural Dynamics* **2016**, *3*, 023605; b) J. K. McCusker, *Accounts of Chemical Research* **2003**, *36*, 876-887; c) R. Bertoni, M. Lorenc, A. Tissot, M. L. Boillot and E. Collet, *Coordination Chemistry Reviews* **2015**, *282-283*, 66-76.
[28] A. Marino, P. Chakraborty, M. Servol, M. Lorenc, E. Collet and A. Hauser, *Angewandte Chemie-International Edition* **2014**, *53*, 3863-3867.
[29] a) R. Bertoni, M. Lorenc, H. Cailleau, A. Tissot, J. Laisney, M. L. Boillot, L. Stoleriu, A. Stancu, C. Enachescu and E. Collet, *Nat Mater* **2016**, *15*, 606-610; b) R. Bertoni, M. Lorenc, T. Graber, R. Henning, K. Moffat, J. F. Létard and E. Collet, *CrystEngComm* **2016**, *18*, 7269-7275.
[30] W. Gawelda, V. T. Pham, M. Benfatto, Y. Zaushitsyn, M. Kaiser, D. Grolimund, S. L. Johnson, R. Abela, A. Hauser, C. Bressler and M. Chergui, *Physical Review Letters* **2007**, *98*, 057401.
[31] V. Briois, P. Sainctavit, G. J. Long and F. Grandjean, *Inorganic Chemistry* **2001**, *40*, 912-918.
[32] N. Huse, H. Cho, K. Hong, L. Jamula, F. M. F. de Groot, T. K. Kim, J. K. McCusker and R. W. Schoenlein, *Journal of Physical Chemistry Letters* **2011**, *2*, 880-884.
[33] E. Biasin, T. B. van Driel, K. S. Kjær, A. O. Dohn, M. Christensen, T. Harlang, P. Chabera, Y. Liu, J. Uhlig and M. Pápai, *Physical Review Letters* **2016**, *117*, 013002.
[34] E. Collet, M. Lorenc, M. Cammarata, L. Guerin, M. Servol, A. Tissot, M. L. Boillot, H. Cailleau and M. Buron-Le Cointe, *Chemistry-a European Journal* **2012**, *18*, 2051-2055.
[35] C. Sousa, C. de Graaf, A. Rudavskyi, R. Broer, J. Tatchen, M. Etinski and C. M. Marian, *Chemistry-a European Journal* **2013**, *19*, 17541-17551.
[36] R. Bertoni, M. Cammarata, M. Lorenc, S. F. Matar, J. F. Letard, H. T. Lemke and E. Collet, *Acc Chem Res* **2015**, *48*, 774-781.
[37] G. D. Scholes, G. R. Fleming, L. X. Chen, A. Aspuru-Guzik, A. Buchleitner, D. F. Coker, G. S. Engel, R. van Grondelle, A. Ishizaki, D. M. Jonas, J. S. Lundeen, J. K. McCusker, S. Mukamel, J. P. Ogilvie, A. Olaya-Castro, M. A. Ratner, F. C. Spano, K. B. Whaley and X. Zhu, *Nature* **2017**, *543*, 647-656.
[38] S. E. Canton, K. S. Kjaer, G. Vanko, T. B. van Driel, S. I. Adachi, A. Bordage, C. Bressler, P. Chabera, M. Christensen, A. O. Dohn, A. Galler, W. Gawelda, D. Gosztola, K. Haldrup, T. Harlang, Y. Z. Liu, K. B. Moller, Z. Nemeth, S. Nozawa, M. Papai, T. Sato, T. Sato, K. Suarez-Alcantara, T. Togashi, K. Tono, J. Uhlig, D. A. Vithanage, K. Warnmark, M. Yabashi, J. X. Zhang, V. Sundstrom and M. M. Nielsen, *Nature Communications* **2015**, *6*, 6359.
[39] S. Zerdane, M. Cammarata, L. Balducci, R. Bertoni, L. Catala, S. Mazerat, T. Mallah, M. N. Pedersen, M. Wulff, K. Nakagawa, H. Tokoro, S.-i. Ohkoshi and E. Collet, *European Journal of Inorganic Chemistry* **2018**, *2018*, 272-277.
[40] K. Pande, C. D. M. Hutchison, G. Groenhof, A. Aquila, J. S. Robinson, J. Tenboer, S. Basu, S. Boutet, D. P. DePonte, M. Liang, T. A. White, N. A. Zatsepin, O. Yefanov, D. Morozov, D. Oberthuer, C. Gati, G. Subramanian, D. James, Y. Zhao, J. Koralek, J. Brayshaw, C. Kupitz, C. Conrad, S. Roy-Chowdhury, J. D. Coe, M. Metz, P. L. Xavier, T. D. Grant, J. E. Koglin, G. Ketawala, R. Fromme, V. Šrajer, R. Henning, J. C. H. Spence, A. Ourmazd, P. Schwander, U. Weierstall, M. Frank, P. Fromme, A. Barty, H. N. Chapman, K. Moffat, J. J. van Thor and M. Schmidt, *Science* **2016**, *352*, 725-729.

.

**Entry for the Table of Contents** (Please choose one layout)

## CONCEPT

Light-induced phenomena result from ultrafast and coupled electronic and structural reorganisations, which may occur beyond the Born–Oppenheimer approximation. The incredibly short and ultra-bright X-ray pulses delivered by X-ray free electron lasers (X-FEL) allow through various techniques gathering new insight into electronic and structural dynamics during light-induced phenomena for a better understanding and control of photoactivated molecular functions.

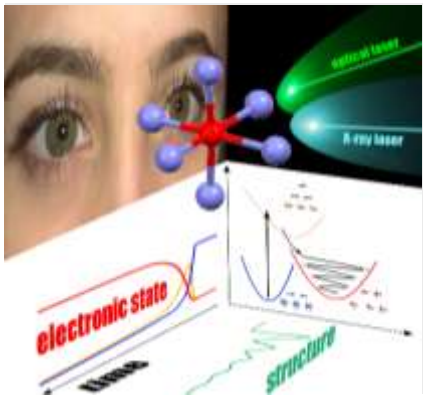


*Eric Collet and Marco Cammarata**

***Page No. – Page No.***

**Disentangling ultrafast electronic and structural dynamics with X-ray lasers**